Title

Dynamic equation-based thermo-hydraulic pipe model for district heating and cooling systems

Authors

van der Heijde, B
Fuchs, M
Tugores, C Ribas
et al.

Publication Date

2017-11-01

DOI

10.1016/j.enconman.2017.08.072

Peer reviewed

Energy Conversion and Management 151 (2017) 158–169

Contents lists available at ScienceDirect

Energy Conversion and Management

journal homepage: www.elsevier.com/locate/enconman

Dynamic equation-based thermo-hydraulic pipe model for district heating and cooling systems

B. van der Heijde[a,b,c,*], M. Fuchs[d], C. Ribas Tugores[e,1], G. Schweiger[f], K. Sartor[g], D. Basciotti[h], D. Müller[d], C. Nytsch-Geusen[e], M. Wetter[i], L. Helsen[a,b]

[a] EnergyVille, Genk, Belgium
[b] KU Leuven, Department of Mechanical Engineering, Leuven, Belgium
[c] VITO NV, Mol, Belgium
[d] RWTH Aachen University, E.ON Energy Research Center, Institute for Energy Efficient Buildings and Indoor Climate, Aachen, Germany
[e] Berlin University of the Arts, Institute for Architecture and Urban Planning, Berlin, Germany
[f] AEE – Institute for Sustainable Technologies, Gleisdorf, Austria
[g] University of Liège (ULg), Thermodynamics Laboratory (B49), Liege, Belgium
[h] Austrian Institute of Technology (AIT), Vienna, Austria
[i] Lawrence Berkeley National Laboratory, Berkeley, CA, USA

ARTICLE INFO

Keywords:
District heating and cooling
Heat loss
Dynamic thermo-hydraulic model
Modelica
District energy systems
Simulation
Thermal network

ABSTRACT

Simulation and optimisation of district heating and cooling networks requires efficient and realistic models of the individual network elements in order to correctly represent heat losses or gains, temperature propagation and pressure drops. Due to more recent thermal networks incorporating meshing decentralised heat and cold sources, the system often has to deal with variable temperatures and mass flow rates, with flow reversal occurring more frequently. This paper presents the mathematical derivation and software implementation in Modelica of a thermo-hydraulic model for thermal networks that meets the above requirements and compares it to both experimental data and a commonly used model. Good correspondence between experimental data from a controlled test set-up and simulations using the presented model was found. Compared to measurement data from a real district heating network, the simulation results led to a larger error than in the controlled test set-up, but the general trend is still approximated closely and the model yields results similar to a pipe model from the Modelica Standard Library. However, the presented model simulates 1.7 (for low number of volumes) to 68 (for highly discretized pipes) times faster than a conventional model for a realistic test case. A working implementation of the presented model is made openly available within the IBPSA Modelica Library. The model is robust in the sense that grid size and time step do not need to be adapted to the flow rate, as is the case in finite volume models.

1. Introduction

In the transition towards a sustainable energy provision, one of the proposed concepts towards higher energy efficiency and the inclusion of renewable energy sources is the new 4GDH system (4th generation district heating and cooling) [1]. These systems are characterised by lower temperature differences, but also intermittent operation, multiple supply temperatures and higher fluctuation of the supply temperature than in conventional systems. These lower temperatures for heating, or higher temperatures for cooling allow for a larger take-up of renewable heat and cold sources such as solar thermal panels, heat pumps, geothermal sources, and industrial waste heat utilisation [2,3].

The variability of local and centralised renewable heat sources alongside new concepts like Active Demand Response, multiple supply temperature levels and reversing mass flows put more requirements on accurate and fast dynamic modelling. More complex system interactions in multi-energy district or even city-wide energy systems necessitate an integrated modelling framework. Schweiger et al. [4] and Böttger et al. [5] have identified a high potential for *power-to-heat* technologies in district heating systems, which would require a more sophisticated pipe model for simulation and control as presented in this work. Not only the physical processes need to be modelled, but also the control of the system.

This brings about a need for high-performance models of all system

* Corresponding author at: EnergyVille, Thor Park, Poort Genk 8310, 3600 Genk, Belgium.
E-mail address: Bram.vanderHeijde@kuleuven.be (B. van der Heijde).
[1] Current address: AEE – Institute for Sustainable Technologies, Gleisdorf, Austria.

http://dx.doi.org/10.1016/j.enconman.2017.08.072
Received 1 July 2017; Received in revised form 18 August 2017; Accepted 27 August 2017
Available online 07 September 2017

Nomenclature

Subscripts

$\square_0$	initial
$\square_b$	boundary
$\square_c$	casing
$\square_g$	ground
$\square_{in}$	inlet
$\square_{mea}$	measured
$\square_{out}$	outlet
$\square_p$	pipe
$\square_{pro}$	production side
$\square_{sim}$	simulated
$\square_{sub}$	substation side

Symbols

A	area (m^2)
C	heat capacity per meter (J/m K)
c_v	specific heat capacity (J/kg K)
f	Darcy friction coefficient (–)
k	thermal conductivity (W/m K)
L	length of the pipes (m)
$\dot{m}$	mass flow rate (kg/s)
p	pressure (Pa)
$\dot{q}$	heat loss rate per meter (W/m)
R	thermal resistance per meter (K m/W)
S	circumference (m)
T	temperature (°C)
U	heat loss coefficient (W/m K)
v	velocity (m/s)
ρ	mass density (kg/m^3)
τ	time constant (s)
ε	relative error (–)

components involved. The goal is threefold: namely high accuracy, low calculation time and high numerical robustness. This paper presents a physical model for district heating and cooling pipes that is able to cope with fluctuating inlet temperatures, varying (even stopping or reversing) mass-flows and arbitrary network lay-outs, including both branching and meshed systems.

This work is done collaboratively within the development of the Annex 60 Modelica Library [6] and the IBPSA Project 1 Modelica Library, which the presented model is contained within. In these international collaborations, the efforts of various research institutes in separate Modelica libraries have been bundled into one free, open-source, validated and well-documented library.

The main contribution of this paper is a novel, open-source, dynamic thermo-hydraulic pipe model for district energy systems.

The aim is to accurately model the thermo-hydraulic behaviour in district heating and cooling pipes. After the derivation of the thermal propagation equations, the model is implemented in Modelica [7] and validated experimentally. Modelica is an equation-based, object-oriented modelling language that allows simulation of complex dynamic processes in multiple physical domains, including their control. The proposed model is validated against two experimental cases. Furthermore, performance of the model is compared to that of a commonly used model in the Modelica Standard Library [7]. The models are compiled and simulated with Dymola [8].

To the authors' knowledge, there exists no freely available open-source models able to handle this degree of complexity with sufficient accuracy. The presented model intends to fill this gap. Available libraries struggle with accuracy or with applicability to larger multi-domain systems [9,10].

1.1. Literature study

This section provides an overview of previous literature on the topic of dynamic simulation of district heating and cooling pipe systems. The literature survey is organised chronologically and based on modelling strategy.

1.1.1. Early steady-state computational models

One of the first scientific reports about modelling heat losses for pipes buried underground can be found in Franz and Grigull [11]. Using an experimental set-up involving an electrically charged plate to represent the temperature field around a supply and return pipe, they effectively linked the thermal problem to its electrical equivalent. Menyhárt and Homonnay [12] described the steady-state heat loss equations for buried pipes in a concrete casing with a supply and return pipe. The mutual influence of supply and return was not taken into account.

In the late 1980s and early 1990s, scientific progress in the field of geothermal borefields and borehole heat exchangers (Eskilson [13], Bennet et al. [14], Hellström [15] and Claesson and Hellström [16]) was applied to the steady state heat loss calculation of district heating pipe systems in different configurations (Wallentén [17]). Configurations considered were pipes buried in the ground or surrounded by air, and pipes insulated separately and jointly. Wallentén described the accuracy of the results of different multipole expansions with increasing order. The simplest method (i.e. the zero-order multipole expansion) introduced an error of up to 5%, while higher order solutions quickly increased the accuracy.

1.1.2. First dynamic models and operational optimisation

With the development of stronger and cheaper computers, dynamic models for the operation of district heating systems started to be investigated. For dynamic simulations, mostly finite element models (so-called *element models*) were used, where the pipe is spatially discretized in order to compute the temperature propagation and heat losses. The physical process of the flow of water through a pipe can be approached as an advection-diffusion equation with a source or loss term. This equation can efficiently be solved with the QUICK discretization scheme [18]. Notice that in regular operation conditions, the diffusive term in the equation is negligible.

On the other hand, the propagation of water can be modelled by only considering the in- and outlet of the pipe and calculating the output based on the propagation delay. This is the so-called *node method* and was described, together with the element method, by Benonysson [19]. Benonysson et al. [20] presented a case study of an operational optimisation of the supply temperature to a district heating system, with operating cost as the objective function. In this study, the node model was not used, but Benonysson et al. expected that the optimisation would be faster if the node model were used.

A general overview of different modelling approaches for district heating pipes and the errors induced by them was presented by Pálsson et al. [21]. They concluded that the number of floating point operations per time step for the element method scales linearly with the number of discretization elements for the pipe. The node method does not use a discretisation and hence the number of floating point operations remains the same for every pipe. The accuracy of the element method is inversely proportional to the square of the element length, while for the node method it depends only on the Courant number.

Bøhm [22] explored the dynamic behaviour of buried district heating pipes under varying boundary conditions, mostly due to weather changes. A method was presented to calculate the transient heat loss by using the heat loss steady-state theory and identifying the location of an undisturbed ground temperature which is used as boundary condition. The dynamic behaviour of larger district heating systems and the aggregation of multiple branches into a simpler representation was studied by Larsen et al. [23,24]. However, their method cannot deal with meshed networks and assumes proportional distribution of the mass flow over the whole district, which is not applicable to the latest generations of district heating, where lower supply temperatures, reinjection of heat by the consumers into the network and mass flow reversals are common. Vesterlund and Dahl [25] applied an operational optimisation method to a meshed network, where the aggregation method cannot be used. To analyse the system interactions including the consumer side, detailed models without aggregation would be needed.

Further comparative studies between commercial software for district heating and the node model of Benonysson were presented by Gabrielaitiene et al. [26] and Gabrielaitiene [27]. In these studies, the different models were compared with measurement data from various district heating systems.

Sandou et al. [28] presented the results of a model-based predictive controller for a district heating system employing a node-like model for the simulation of the temperature propagation. For control optimisation, a simple, linear relation between the input and output temperatures of the pipes was used in order to limit complexity. However, the simulation model was still used for the verification of the calculated control action and as such, feedback was provided.

1.1.3. Finite volume methods and function methods

A model presented by Stevanovic et al. [29] predicts temperature transients in district heating operation. Their approach is based on the element method, but due to a third order discretization scheme employed for the spatial discretization, no artificial numerical diffusion of temperature steps appears. The model was compared with measurements of a real network. Grosswindhager et al. [30] discussed the numerical behaviour of an adapted version of the finite difference scheme called QUICKEST. QUICKEST is a variation of a third order finite difference scheme. Grosswindhager et al. modified the scheme to cope with changes in diameter, near-zero flow velocity and junctions of multiple pipes in thermal networks. Furthermore, their model can cope with sudden temperature changes more accurately.

Dalla Rosa et al. [31] studied the heat losses from pipe systems with more than two pipes using finite element models of the pipe cross section. They took into account the variation of thermal conductivity with temperature. Furthermore, Dalla Rosa et al. [32] validated an implementation of the node model in MATLAB against a FEM/CFD model in Ansys/Fluent. Again, good correspondence between measurement data, the FEM simulation and the simpler implementation was found.

Ben Hassine and Eicker proposed another variation of the element model implemented in MATLAB [33]. They used this to calculate a case with a meshed network in Germany, although the size of the simulated network was limited in order to avoid overly long calculation times.

Guelpa et al. [34,35] presented a fluid-dynamic model for district heating systems, incorporating pressure drops and heat losses. The heat loss model is based on an upwind scheme, which is then iterated until convergence is reached. They described a method to derive a reduced order model based on proper orthogonal decomposition with radial basis functions, applied to the district heating system of Torino. The proposed method reduced the calculation time by 80% compared to a reference case, while maintaining the necessary accuracy.

Kauko et al. [36] modelled a low temperature district heating system for Trondheim, Norway, using Dymola. The heat loss model employed here is based on that of Dalla Rosa et al. [31]. A significant reduction in heat losses with respect to a high temperature district heating network was concluded.

Function methods model heat losses based on a Fourier analysis of the heat transfer equations and the input temperature profile. An analytical solution to the temperature propagation equations was proposed by Jie et al. [37]. They described the solution for a cyclic input temperature with a period of 24 h, corresponding to a diurnal pattern. The constructed model was applied to a linear network (no meshes or branches) in China and the results were in accordance with measurement data. Zheng et al. [38] applied a similar method to the simulation of a district heating system in Changchun, China, and compared it to the node method in terms of calculation time and accuracy. They found a smaller average error and standard deviation of the error for the function method than for the node method, while the calculation time was also reduced by approximately 37%. The mass flow rate, however, was held constant.

1.1.4. New computational tools and plug flow models

Skoglund et al. [39] and Skoglund and Dejmek [40] described object-oriented models for food processing heat exchangers and fluid food dispersion in turbulent flows using Modelica. To this end, they used a plug-flow approach, imposing the analytical solution of the advection–dispersion equation at the end points of a pipe, while propagating the fluid properties and modelling the advection part with an “ideal” plug-flow pipe.

Velut and Tummescheit [41] proposed to solve a similar flow problem by using a transmission line model (TLM) to represent a single pipe through which a fluid is transported. Again, only the fluid properties at the inlet and outlet of the pipe are of interest here. In order to calculate the temperature drop along the pipe, a partial differential equation for the energy balance is integrated over the length of the pipe. The solution requires the time difference between the entrance and exit of the fluid to/from the pipe. Velut and Tummescheit used a differential equation to track this time delay.

Giraud et al. [42] described a Modelica library for modelling and simulating district heating systems that is based on the specialised functions to model delays and advection processes in Modelica. Using this model library, they optimised the control of variable temperature district heating systems [43]. The scheduling and power of the heat generators, the network supply temperatures and differential pressure were controlled.

Van den Bossche [44] studied the propagation of supply temperature steps in a small-scale district heating network. He proposed a plug-flow modelling approach. It was concluded that the finite volume approach, currently in use in the Modelica Standard Library pipe model, introduces inaccuracies depending on the discretization size. Sartor et al. [45] drew the same conclusions as Van den Bossche [44] in a theoretical study that compares the results of the finite volume approach and the related discretization with a two dimensional computational fluid dynamic simulation. Sartor and Dewallef showed and validated an implementation of a node model considering thermal inertia and heat losses in MATLAB based on a TRNSYS model [46].

A successful implementation of a plug-flow Lagrangian approach was shown by Oppelt et al. [47]. They applied this novel modelling strategy to a single-pipe cooling network. Schweiger et al. [48,49] presented a Modelica-based framework to represent, simplify, simulate and optimise district heating systems as well as a method to decompose a mixed-integer-optimal control problem into two sub-problems, separating the discrete part from the continuous one.

1.2. Research motivation

It can be concluded from the previous studies that modelling heat flows in thermal networks has been studied for a long time, but in the light of the newer network generations, gaps still exist. The accurate representation of heat losses and the correct representation of

temperature waves are two of them. Furthermore, a means of modelling networks both thermally and hydraulically for highly varying circumstances is needed. The application of the newly developed model to different cases in this paper shows that it has potential to be used to a solve a large variety of problems.

2. Methodology

In this section, the model equations and structure are explained. The first part elaborates on the derivation of the heat losses, while the second part focuses on the calculation of the delay time. Thereafter, the thermal inertia calculation is explained, followed by the hydraulic behaviour. Finally, solution methods in Dymola are briefly discussed.

2.1. Heat loss calculation

The transport of energy through the pipes and the associated heat losses to the surroundings are guided by a combination of the energy and continuity equation with the internal energy as a function of the axial position in the pipe x and the time t as:

$$\underbrace{\frac{\partial(\rho c_v T A)}{\partial t}}_{\substack{\text{time}\\ \text{derivative}}} + \underbrace{\frac{\partial\left(\rho v\left(c_v T + \frac{p}{\rho}\right)A\right)}{\partial x}}_{\text{spatial derivative}} = \underbrace{vA\frac{\partial p}{\partial x}}_{\substack{\text{pressure}\\ \text{difference}\\ \text{energy}}} + \underbrace{\frac{1}{2}\rho v^2|v|f_D S}_{\substack{\text{wall friction}\\ \text{dissipation}}} + \underbrace{\frac{\partial}{\partial x}\left(kA\frac{\partial T}{\partial x}\right)}_{\text{axial heat diffusion}} - \dot{q}_e, \tag{1}$$

where ρ denotes the mass density, c_v is the specific heat of the fluid in the pipe, A is the cross section area of the pipe, v is the flow velocity, p is the absolute pressure, x is the spatial coordinate along the length of the pipe, t is the time, f_D is the Darcy friction coefficient, S is the pipe circumference, k is the thermal conductivity, T is the temperature and $\dot{q}_e$ is the heat loss per unit length [7]. $\dot{q}_e$ is positive for heat loss from pipe to surroundings. This equation can be interpreted as an advection equation with a source term $-\dot{q}_e$.

Eq. (1) can be simplified by deleting the negligible terms. The conditions for neglecting diffusive heat transfer in the pipe can be checked using the Péclet number. Van der Heijde et al. [50] verified that heat diffusion can be neglected in most of the operational range of thermal network pipes. The effects of pressure loss, wall friction and the dissipation of these losses as heat are negligible, but could be added to the model without much effort. Rewriting (1) by removing the neglected terms yields:

$$\frac{\partial(\rho c_p A T)}{\partial t} + \frac{\partial(\rho c_p A v T)}{\partial x} = -\dot{q}_e. \tag{2}$$

The heat loss per unit length is assumed to be proportional to the temperature difference between the water in the pipe and the undisturbed ground or ambient. The remainder of this paper uses simple formulas for calculating the thermal resistance of an insulated cylinder, either suspended in air or buried underground. The actual calculation of the equivalent resistance between the water and reference (air or soil) temperature is not explained here, since the remaining derivation of the model equations is independent of the resistance value.

Assuming that axial diffusion is negligible, the temperature change of an element of fluid between inlet and exit depends only on its initial temperature and on its residence time in the pipe. For a double pipe system, there will also be a mutual influence of the temperatures in the two pipes, as studied by van der Heijde et al. [50]. Due to the lack of experimental validation data for this problem, only the single pipe model is treated in the remainder of this paper.

For the study of a single pipe through which water flows, a Lagrangian approach is suggested. In this approach, the observer travels along with a moving fluid parcel.

The heat capacity per unit length of the water in the pipe is $C = Ac_v\rho$. We assume that there is a known thermal resistance per unit of length R between the fluid temperature T and the surroundings at T_b, for example as calculated by Wallentén [17]. The temperature of the fluid is presumed to be uniform throughout the cross section of the pipe (see van der Heijde et al. [50]). The change of the temperature of the material surrounding the water is neglected for now.

Since the observer is attached to the moving fluid parcel, there is no notion of the spatial coordinate at which the parcel is located. Hence, the energy balance equation for a parcel with an infinitesimal length δx can be found as

$$\frac{dCT(t)}{dt}\delta x = -\frac{T(t)-T_b}{R}\delta x. \tag{3}$$

δx appears on the right hand side of the equation as part of the total resistance of the parcel $R/\delta x$. (3) is integrated with respect to dt and dT, where the integration bounds are the inlet and outlet temperatures for variable $T(t)$ and inlet and outlet time for t. The temperature of the surroundings T_b is also variable, but due to the large inertia of the ground, its fluctuation is much slower than the temperature dynamics in the pipe. After rearranging such that the variables are at separate sides of the equation, we obtain:

$$\int_{T_{in}}^{T_{out}} \frac{dT}{T-T_b} = -\frac{1}{RC}\int_{t_{in}}^{t_{out}} dt \tag{4}$$

and hence

$$T_{out} = T_b + (T_{in}-T_b)\exp\left(-\frac{t_{out}-t_{in}}{RC}\right). \tag{5}$$

This is the same result as found by Velut and Tummescheit [41].

In this derivation, no assumptions have been made about flow velocity. Since the solution for the outlet temperature only depends on the time delay $t_{out}-t_{in}$, the velocity can have any profile. However, care must be taken when the flow velocity becomes so small that diffusion cannot be neglected any more.

For the implementation in Modelica, it is assumed that the calculation of the fluid and temperature propagation can be separated from the heat loss calculation. This allows us to use the `spatialDistribution()` operator as defined in the Modelica Language Specification [7] to calculate the advection of fluid through the pipe. At the two ends of the pipe, the heat loss and temperature drop are calculated based on the propagation time, the temperature of the fluid when it entered the pipe and the boundary conditions.

The heat loss calculation takes into account the flow direction. Only the heat loss component at the outlet of the pipe, relative to the current flow direction, is active, while the opposite component just passes the fluid into the pipe.

2.2. Delay time

In order to know the delay time of any fluid parcel in the pipe, its inflow time t_{in} is stored and compared to the current simulation time when the fluid leaves the pipe. Hence, t_{in} is considered as a property of the fluid. Fluid properties that are transported through the pipe, such as enthalpy, can be described by the one-dimensional wave equation,

$$\frac{\partial z(x,t)}{\partial t} + v(t)\frac{\partial z(x,t)}{\partial x} = 0, \tag{6}$$

where $z(x,t)$ is the transported quantity. The solution of the one-dimensional wave equation will be approximated using the `spatialDistribution()` operator.

The advantage of the `spatialDistribution()` operator is that it can easily cope with zero flow and flow reversal. Although the differential equation that Velut and Tummescheit [41] used would yield comparable results, it has the difficulty that the time delay must be

reinitialized every time after zero-flow, which is circumvented with this method.

2.3. Thermal inertia

To account for the thermal inertia of the pipe wall, thermal capacities are added to the pipe model. Due to the linearity of the thermal calculations, the location of this capacity at the inlet or outlet of the pipe does not matter, as long as the flow direction remains constant. When flow reverses, e.g., at t^* where $\lim_{t\to t^*-}\dot{m}(t)\cdot\lim_{t\to t^*+}\dot{m}(t) < 0$, an assessment for each fluid parcel would be necessary. However, this is a shortcoming that will only have a limited effect, since the thermal capacity of the pipe wall is usually smaller than that of the water flowing through it.

In the Modelica implementation, the thermal capacity of the pipe wall is represented by a single capacitance per pipe segment, located at the outlet of the pipe, i.e. under design flow direction. Benonysson [19] used the same approach. The thermal capacity of the pipe wall is represented as an equivalent water mixing volume. Apart from approximating the correct thermal dynamic behaviour, this volume hydraulically separates adjacent pipes, thus simplifying the pressure calculations by avoiding systems of nonlinear equations.

2.4. Hydraulic behaviour

Hydraulics in the model are based on the `HydraulicDiameter`[2] model from the Annex 60 library [6], currently developed as the IBPSA Project 1 library. The pressure drop is linked to the mass flow rate using a quadratic relation with a fixed proportionality constant K, which is calculated from the pipe equivalent length and the pressure drop during nominal conditions. Below the critical Reynolds number, the function is regularized in the neighbourhood of zero mass flow rate in order to make it twice differentiable. Otherwise, the derivative of the mass flow rate with respect to the pressure difference would not exist at zero flow rate (see Wetter et al. [6]).

2.5. Solution methods

The model described in this section is implemented in Modelica and compiled and simulated in Dymola. This software package compiles the Modelica code into executable `C` code according to the selected solution method. Different solver choices are available, ranging from Euler, second and fourth order Runge–Kutta, Dassl (Petzold solver) etc. In the results hereafter the Dassl solver is always chosen. Further discussion of the solution methods is outside the scope of this paper.

3. Experimental validation

This section discusses the experimental validation of the proposed model for a single pipe segment.

3.1. Experimental set-up

The experimental set-up at the Thermodynamics Laboratory of the University of Liège (ULg), shown in Fig. 1, is composed of one 39 m single steel pipe. The design of the test bench allows studying the influence of flow velocity and inlet temperature steps on the outlet temperature.

The pipe has an inner diameter of 52.48 mm, a wall thickness of 3.9 mm and is surrounded by 13 mm insulation. Its thermal conductivity is 0.04 W/(m K). The density of the pipe wall is 8000 kg/m^3 and its specific heat capacity is assumed to be 500 J/(kg K) [51]. Natural convection from the outer surface of the pipe to the surrounding air is approximated by a heat transfer coefficient of 4 W/(m^2 K) [52].

The ambient temperature near the pipe is measured by a type T thermocouple, which is shielded to prevent radiation influence. Inlet and outlet water temperatures are measured by type T thermocouples directly immersed inside the pipe to avoid measurement delay usually caused by immersion sleeves. Due to test bench constraints, the maximum flow velocity considered is 1 m/s. In a typical district heating network, the flow velocity is generally lower than 2 m/s [53–55] to limit pressure losses.

The inflowing water is heated by a modulating 350 kW natural gas boiler and the volume flow rate is measured by a mechanical volume flow meter with pulse counter (4 pulses per litre) with a nominal volume flow rate of 6 m^3/h. Temperature steps are obtained by means of modulating the power output of the boiler. The inlet temperature of the pipe was measured and these measurements are used directly as an input to the simulations. Before each test, the pipe was flushed with water from the city's water supply system for about 10 min to bring the system to steady-state. Hereafter, the boiler was switched on and the water was heated until the desired inlet temperature was reached.

The data acquisition system is a National Instruments (NI) cDAQ 9188 coupled with an NI9213 card to read out the thermocouple measurements and an NI9401 card for pulse counting. Table 1 lists the accuracy of each sensor. The temperature measurements have been rounded off to one decimal place.

A number of experiments have been performed with various mass flow rates and temperature steps, as described in Table 2. T_0 indicates the initial temperature of the water at the inlet of the pipe, while T_{max} is the maximal water inlet temperature during the experiment. The temperature evolution during all of the experiments is represented in Figs. 2–5. During each of the experiments, the mass flow rate was kept constant. The experimental data can be accessed in the Annex 60 repository[3] by the respective data set names.

All of the cases presented in Table 2 use the measured inlet temperature profile of the pipe and the indicated mass flow rate as input. The fluid temperature inside the pipe is initialized as a linear interpolation between the measured inlet and outlet temperatures at the start of the test. The time delay is initialized using the fixed mass flow rate of each experiment.

The root mean square error of the simulated outlet temperature T_{sim} with respect to the measured outlet T_{mea} is calculated as

$$RMSE = \sqrt{\frac{1}{n}\sum_{i=1}^{n}(T_{mea,i}-T_{sim,i})^2}, \tag{7}$$

where n is the number of measurement points.

3.2. Results

Figs. 2–5 show three lines in the upper graph; the simulated and measured output are shown solid, and the dashed line shows the delayed input. This is the temperature that would be measured at the outlet without heat losses, without heat transfer in the axial and radial direction, with perfect plug flow and without thermal inertia, i.e. only considering the temperature propagation. In the lower graphs, the difference between measurement and simulation is plotted in terms of outlet temperature and heat loss. The dashed red line shows the measurement error given the accuracy of the thermocouples (see Section 3.3).

Experiments A and B investigate the influence of the pipe's heat losses and thermal inertia on the outlet temperature for two water velocities (~ 0.3 and 1 m/s) which are typically encountered in the ULg district heating network. The influence of heat losses is correctly represented by the model. The thermal inertia of experiment A (Fig. 2) is also approximated well, except for an underestimation of the inertia at

[2] See model `IBPSA.Fluid.FixedResistances.HydraulicDiameter`.

[3] Openly accessible via https://github.com/ibpsa/modelica-ibpsa.

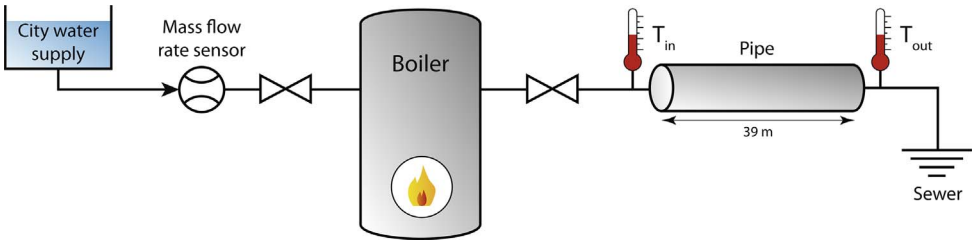

Fig. 1. Test rig diagram.

Table 1
Accuracy and ranges of the sensors used on the test rig.

Sensor	Accuracy	Range
Type T thermocouple	0.3 °C	−40 to 120 °C
Volume flow rate	3%	0.48–12 m^3/h
NI9213	0.6 °C	–

Table 2
Conditions of experiments for one single pipe.

Exp.	Data set	T_0 [°C]	T_{max} [°C]	$\dot{m}$ [kg/s]
A	PipeDataULg151202	18	52	0.589
B	PipeDataULg160118_1	18	39	2.269
C	PipeDataULg151204_4	28	60	1.257
D	PipeDataULg160104_2	15	35	0.249

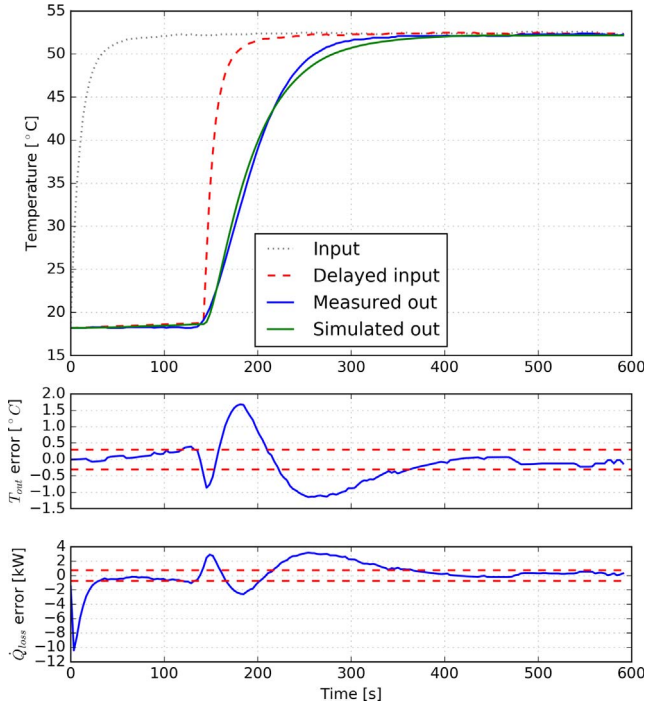

Fig. 2. The validation results for Experiment A (water velocity: 0.3 m/s) show good agreement between measurements and simulation. The red dashed lines in the lower two plots mark the accuracy of the temperature measurements and of the difference in heat losses. (For interpretation of the references to colour in this figure legend, the reader is referred to the web version of this article.)

the beginning of the temperature increase, followed by a slight overestimation toward the steady-state at about 50 °C.

Experiment B is characterised by a higher water velocity, which is translated to a smaller delay time in Fig. 3 compared to Fig. 2. Here the simulated outlet temperature rises faster than the measurements during

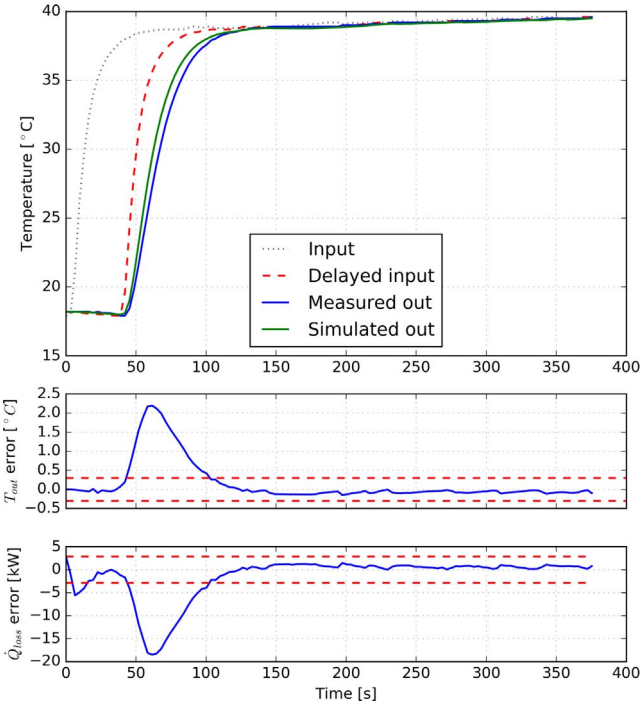

Fig. 3. In Experiment B, the highest flow velocity (water velocity: 1 m/s) was tested, resulting in relatively high deviations during the temperature transition.

the whole temperature step, followed by a nearly zero, but slightly negative error.

Experiment C (Fig. 4) is characterised by an upward temperature step followed by a downward step, which corresponds better to situations encountered in a real thermal network. The thermal inertia is underestimated as for Experiment B. This underestimation leads to a slightly faster temperature change than measured. The fact that the temperature error is the same for B and C, while the mass flow rates are different, could be explained by the difference in temperature step. A higher temperature step would most likely lead to a higher error.

Experiment D (Fig. 5) studies a low water flow velocity of around 0.12 m/s, combined with a gradual temperature change. During the temperature increase, the simulated output seemingly lags about 20 s behind the measurement, compared to a total transport delay of 330 s. During the temperature decrease, the temperature delay between measurement and simulation is less than 5 s, but now in the other direction, i.e. the measurements seem to lag behind the simulations. The temperature discrepancy between simulation and measurements, however, stays within the measurement accuracy for most of the time.

Table 3 shows the error statistics for the different experiments. The initialization period has been disregarded in the calculation of these statistics in order to only account for the relevant model error.

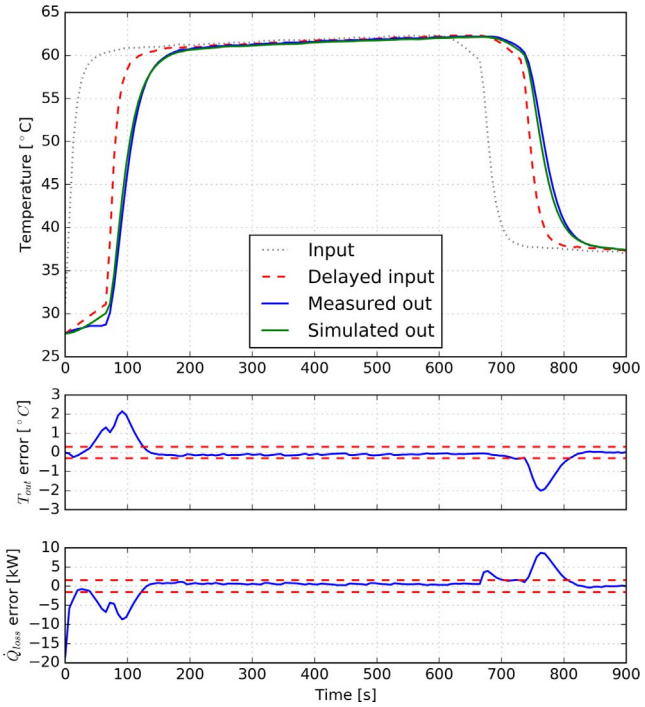

Fig. 4. Experiment C is characterised by two temperature steps in opposite direction. The intermediate water velocity (water velocity: 0.64 m/s) results in errors that are larger than is to be expected from the accuracy of the temperature sensor, but lower than for Experiment B.

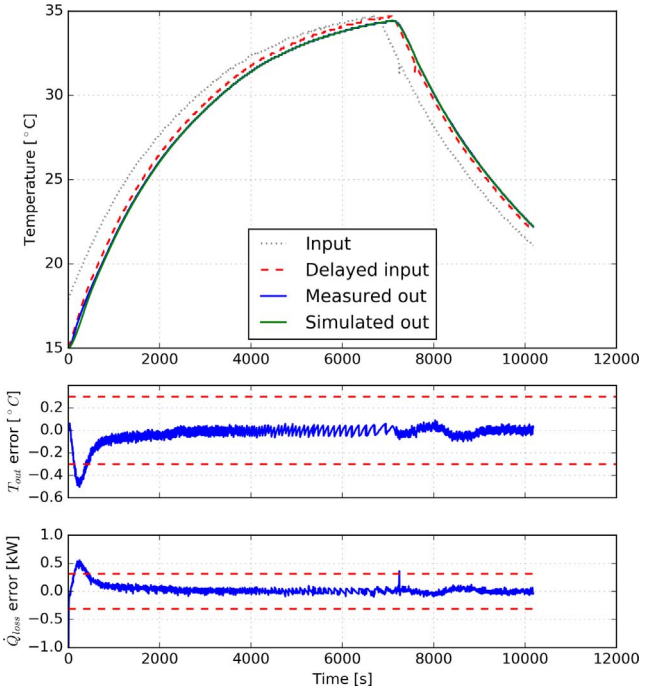

Fig. 5. The simulation results of experiment D, characterised by a gradual temperature change (water velocity: 0.12 m/s), fit very well to the measurement data. Outlet temperature and heat losses are within their respective accuracy bounds for most of the time. The jagged error lines are a result of rounding of the measurement data to reflect the measurement accuracy.

3.3. Discussion

The model seems to slightly underestimate the thermal inertia for high water velocity, but overestimates it when the water velocity is lower. This behaviour can be explained by the assumption of a single capacity to represent the whole pipe, whereas a discretized pipe can achieve slightly more accurate results. Furthermore, it is expected that axial mixing and diffusion do have a small yet noticeable influence, contrary to the assumptions in the model. However, there is a good agreement between the model and the experimental data for the outlet pipe temperature.

Table 3
Root mean square error (RMSE), average error and standard deviation of the error for the simulations and measurements from the single pipe experiments.

Experiment	RMSE [°C]	Avg. error [°C]	Std. dev. [°C]
A	0.65	−0.14	0.286
B	0.60	0.17	0.573
C	0.56	−0.11	0.551
D	0.10	−0.09	0.055

Another explanation for the inaccuracy during temperature steps could be due to slight discrepancies in the mass flow rate measurement. Indeed, varying the mass flow rate within the accuracy range of the meter often leads to better correspondence between the two temperature evolutions. Finally, the temperature of the test rig's surroundings is assumed to be constant at 18 °C. Variations of this temperature could also explain part of the discrepancy in Experiment D.

Figs. 2–5 also show the difference in heat losses between the simulation and measurements. For convenience, the minimal discernable heat loss is also shown on the graph using dotted red lines. Within this band, the difference in heat losses can be attributed to temperature measurement inaccuracies at a constant mass flow rate:

$$\dot{Q}_{min} = c_p |\Delta T_{min} \dot{m}|. \tag{8}$$

The heat losses remain well within the accuracy band, except for when a temperature step travels through the pipe. Then, the heat loss difference between simulations and measurements rises just as the temperature errors do. Again, the initialization phase is not accounted for because of lack of information on the initial state of the water in the pipe.

While the root mean square error (see Eq. (7)) is about twice the measurement accuracy except for Experiment D, the average error is well below this accuracy. Experiment D shows a particularly good fit, which is believed to originate from the smoother changes in temperature in this experiment. In these results, the discrepancy between measurements and simulation most likely originates from a small inaccuracy in the pipe dimensions and material properties. This presumption is additionally confirmed by the steady state temperature error in Experiments B and C, whose value is slightly below zero.

It is remarkable that the model performs well with only a few geometric parameters, namely the diameter, insulation thickness and an approximative heat conduction coefficient. This corroborates the robustness and simplicity of the presented plug flow model.

4. Comparison with discretized pipe model

This section shows the application of the presented model to a real case study and serves to discuss and validate its performance. The plug flow model's results are compared to that of a commonly used model, namely the dynamic pipe model (`Modelica.Fluid.Pipes.DynamicPipe`) from the Modelica Standard Library (MSL) version 3.2.2.[4]

4.1. Case description

The test case is a part of a district heating network in Pongau, Austria. The network topology and its lengths are represented

[4] Accessible from http://doc.modelica.org/.

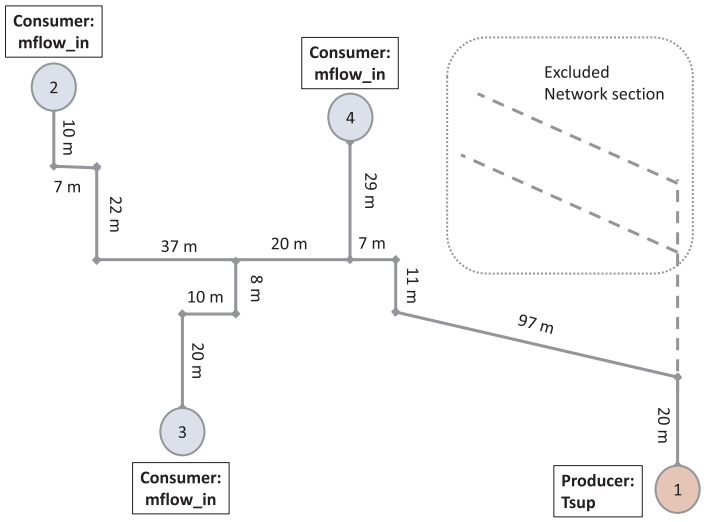

Fig. 6. Schematic representation of the considered district heating network in Pongau (Austria).

schematically in Fig. 6. All main pipes are of type DN80, with further technical details summarised in Table 4. The pipes from the main line to the substations are of type DN25, but without further information about the amount of insulation. Two main branches depart from the producer: one supplies the three studied consumers, the other connects a part of the network that is excluded from the study. Measurements are taken for the supply temperature and mass flow rate at the producer and three consumers. The measurements are taken during a winter week.

Because the pipes are buried at about one meter depth, the heat resistance of the soil has to be considered. The overall thermal resistance of the pipe per unit length R is the sum of the heat resistance of soil and pipe:

$$R = \frac{1}{2\pi\lambda_i}\ln\left(\frac{d_c}{d_o}\right) + \frac{1}{2\pi\lambda_g}\ln\left(\frac{2H}{d_c}\right), \tag{9}$$

where $d_c = d_o + 2s_i$ is the diameter of the pipe casing, assuming a thermal conductivity for the ground λ_g of 2.4 W/(m K), the overall thermal resistance per unit length R is 4.92 m K/W for the DN80 pipes. For the DN25 pipes between the main line and the customers, a jacket pipe (diameter outside insulation) of 70 mm is chosen, in the absence of more specific information about the installed pipes.

The MSL model is a finite volume model and the number of segments n per pipe is chosen to be one element per meter. For a second comparison, a rougher discretization of only two elements per pipe segment is chosen. For this implementation, one thermal resistance is used. All elements of one pipe have equal length. The IBPSA Modelica Library model for liquid water with constant density (`IBPSA.Media.Water`) is used in all models.

The same Dassl solver and simulation tolerance (1×10^{-5}) are used in both cases. The first 6 h of the simulation results are affected by initialization of the model and therefore omitted.

The supply temperature of the source varies between 90 °C and 105 °C, see Fig. 7. The data shows fluctuating mass flow rate at the substations, especially at substation 2, with periods of zero mass flow rate at the substation 4.

Table 4
Technical details of pipes in test case.

Dimensions	DN80	DN25
Inner diameter d_i	0.0825 m	0.0273 m
Outer diameter d_o	0.0889 m	0.0337 m
Insulation thickness s_i	0.045 m	0.0182 m
Buried depth H	ca. 1 m	ca. 1 m
Insulation parameters	Both	
Material	Polyurethane	
Heat conductivity (average at 50 °C)	0.024 W/(m K)	

4.2. Results

The simulation results at substations 2 and 3 (Fig. 8a and b) show how both pipe models match with the temperature profile of the measured data. Slight temperature and timing differences are apparent, but this is to be expected from the uncertainty on the measurements. The first six hours are not shown because the simulation is still initializing.

Nevertheless the heat transfer coefficients tend to be underestimated, mostly for substation 2. Such underestimation might be explained by the uncertainty related to the definition of the heat loss coefficient. The influence of insulation material ageing, as discussed by Kristjansson and Bøhm [56] and De Boer et al. [57] is not taken into account, and neither is the temperature dependency of the thermal conductivity. On the other hand, the assumption of a relatively high thermal conductivity of the soil might have partially compensated these

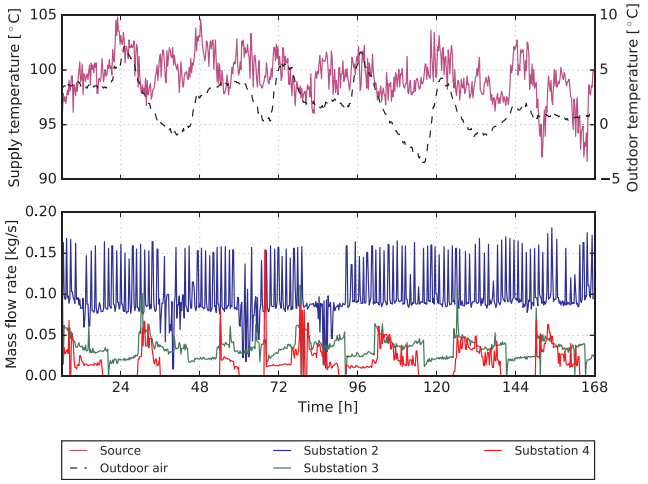

Fig. 7. Input data. Upper graph: supply temperature to the network (solid magenta, left scale) and outdoor air temperature (dashed black, right scale). Lower graph: mass flow rate at the three substations. Notice zero flow periods at substation 4. (For interpretation of the references to colour in this figure legend, the reader is referred to the web version of this article.)

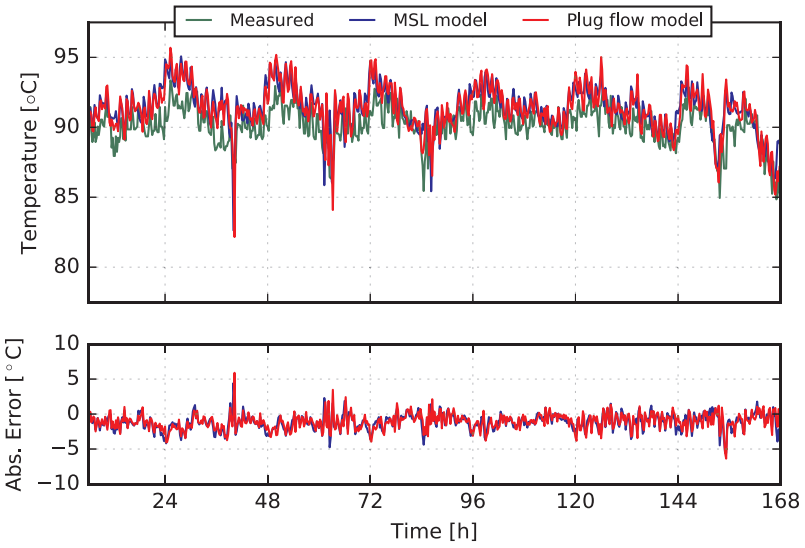

(a) Substation 2

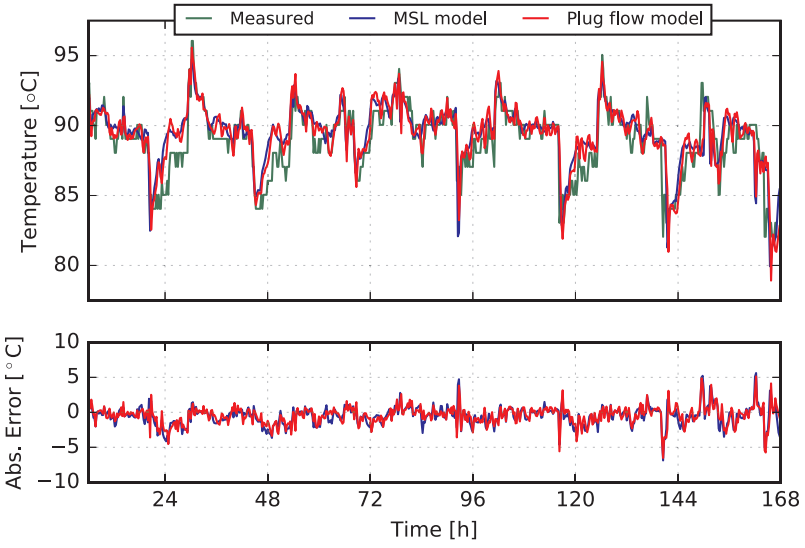

(b) Substation 3

Fig. 8. The simulation results with MSL and plug-flow model for substations 2 and 3 show that both models yield similar results, and are approximately equally offset from the measurement data.

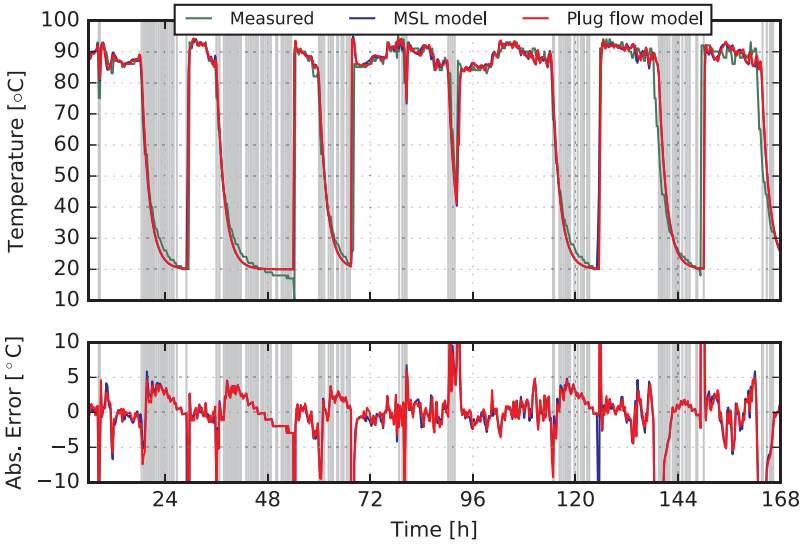

Fig. 9. The behaviour of both models after periods of zero flow (shaded in grey) is shown for substation 4. Again, both models yield very similar results.

Table 5
Temperature relative error ε, temperature average error and its standard deviation for the three considered consumers of the test network.

Subs.	MSL model (1/m)		MSL model (2/pipe)		Plug flow model	
	ε [–]	Avg. err. [°C] (std. dev.)	ε [–]	Avg. err. [°C] (std. dev.)	ε [–]	Avg. err. [°C] (std. dev.)
2	−0.11	1.05 (1.34)	−0.11	1.13 (1.15)	−0.12	1.10 (1.15)
3	−0.01	0.40 (1.52)	−0.02	0.53 (1.36)	−0.02	0.46 (1.29)
4	0.06	0.33 (8.74)	0.06	0.46 (8.65)	0.06	0.37 (8.55)

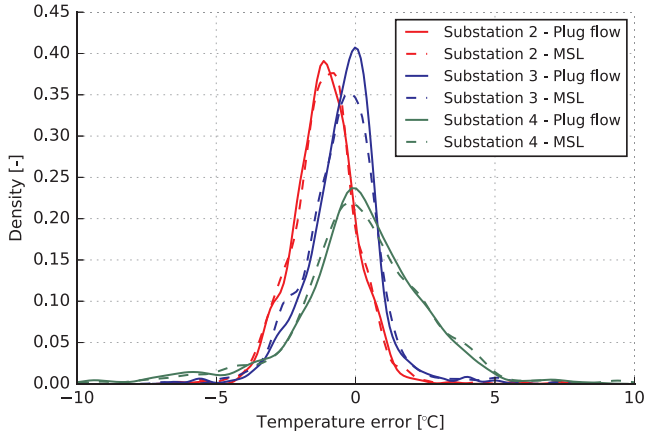

Fig. 10. Error density plot of all substations for plug flow (solid) and MSL model (dashed lines). Both models show comparable accuracy, with a slightly lower standard deviation for the plug flow model in the studied error range. The mean error of substation 2 shows that both models have a systematic offset as a result of incorrect input parameters.

Table 6
Model complexity statistics of plug flow and MSL models.

	MSL (1/m)	MSL (2/p)	Plug flow
Original			
Number of components	1569	145	228
Unknowns	9901	1035	1659
(of which scalars)	22,838	1102	1288
Differentiated variables	899	41	29
Equations	6007	859	1267
Translated			
Continuous time states	303	17	23
Time-varying variables	4252	242	355
Alias variables	8733	445	767
Sizes of lin. systems of equations	{ }	{ }	{ }
After manipulation of lin. sys.	{ }	{ }	{ }
Sizes of nonlin. systems of equations	292 × {1}	{1, 1, 1, 1, 1, 1}	{ }
After manipulation of the nonlin. sys.	292 × {1}	{1, 1, 1, 1, 1, 1}	{ }
Number of numerical Jacobians	0	0	0

simplifications.

The results for the temperature profile at substation 4 (Fig. 9) clearly match the measured data for periods of normal operation. There are some misalignments after and before flow standstill, but both the MSL and plug flow pipe results show the same error so the reason is expected to be due to measurement inaccuracies.

The temperature measurements are simulated using a model for a temperature sensor with a non-zero time constant. This means that when the mass flow rate is zero, the sensor (and the water in the pipe) gradually cools down to ambient temperature. This cooling effect is needed in the case of the plug flow model, since it can only correctly represent the outlet temperature and heat losses of the pipe after the flow has started in either direction again. As long as the flow rate remains at zero, the water temperature at both pipe inlets and outlets stays constant. For fair comparison, the same temperature sensor is used in the MSL implementations. From the measurement,s it is clear that the surroundings are not at a constant temperature, but for simplicity a temperature of 20 °C was assumed for the simulations. The time constant of this cooling process was tuned so as to approximate the cooling behaviour at zero flow appropriately. After the water flow starts again, the actual outlet temperature is recalculated using the presented model.

In order to assess the quality of the models, three parameters, analogous to the ones described by Gabrielaitiene [27] are used: the average error calculated as the difference between simulated and measured temperature at each substation, the standard deviation of the average error and a relative error ε of the temperature prediction at the substations, calculated as

$$\varepsilon = \frac{(T_{pro}-T_{sub})_{sim}-(T_{pro}-T_{sub})_{mea}}{(T_{pro}-T_{sub})_{mea}}, \tag{10}$$

where the subscripts stand for production *pro*, consumer or substation *sub*, simulated *sim* and measured *mea*.

A summary of the errors for both used models is presented in Table 5. To avoid distorting the value of these parameters, only meaningful values were taken into account, hence the first 6 h as well as any period of zero mass flow rate are disregarded. In addition, Fig. 10 shows the approximate error density plots at all substations and for both models within the error range [−10 °C, 10 °C]. This shows that both models perform more or less equally, with a slightly lower standard deviation for the plug flow model in the considered error range. Substation 4 is shown to have a larger deviation than the other two substations. This figure also confirms the systematic deviation of the simulation results in Substation 2.

The small relative errors indicate that both models perform similarly and adequately regarding the simulated temperatures. The negative sign confirms the observed underestimation of the heat losses. The plug flow model has slightly larger average errors than the highly discretized MSL model (1/m in Table 5), but the standard deviation is slightly lower. This shows that the accuracy of both models is comparable. The MSL model with only two elements per pipe (2/p) also shows similar statistics, although the average error is slightly larger than the previous two.

Furthermore, the model complexities of the plug flow model and both of the MSL model discretizations are compared in Table 6. Empty curly brackets "{ }" denote the absence of a linear or nonlinear system. The notation of a number *x* times {1} means that there are *x* nonlinear systems of size 1. The plug flow model stands out because of the absence of nonlinear systems, as a result of the pressure state between each pipe. The MSL implementation with two elements per pipe (2/p) appears to be the least complex when comparing most of the other statistics.

Based on 50 consecutive runs of each of the implementations of the case in Pongau, the plug flow model has the lowest translation and simulation time, closely followed by the MSL pipe model implementation with 2 elements per pipe (see Fig. 11). The plug flow implementation has an average CPU time of 1.92 s, the MSL with 2 elements per pipe of 3.25 s. These two implementations largely outperform the MSL pipe model with one element per meter, which averages at a translation and simulation time of 130.25 s, i.e. 68 times slower than the plug flow model on average. These results were compared on a Dell Latitude E7470 device with an Intel® Core™ i7-6600U 2.60 GHz with 2 cores (4 logical processors), of which one was used for each simulation; the device has 16 GB RAM and runs Windows 10 as operating system. Dymola 2017 FD01 was used with a Visual C++ 2015 express edition (14.0) compiler.

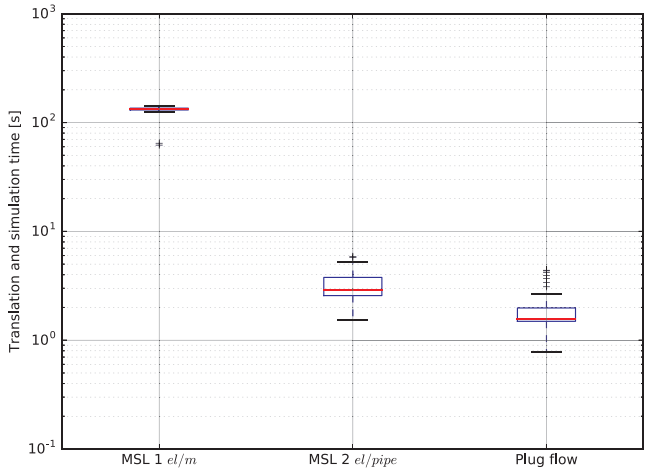

Fig. 11. Boxplot of the CPU times of 50 runs of the three network implementations compared. The plug flow model is the fastest, closely followed by the MSL model with the minimum discretization.

4.3. Discussion

The temperature profile of the MSL pipe shows a slightly smoother temperature trajectory than the presented pipe model (see for instance Fig. 8b). This can be explained by the discretized approach used by the MSL pipe. The pipe is segmented along the length into fluid volumes that are assumed perfectly mixed based on the interaction with neighbouring elements. This approach introduces artificial numerical diffusion, which smoothens the propagated temperature, whenever the grid and time step are not adapted to the flow velocity. The smoother temperature behaviour is expected to originate from this effect.

In order to make a fair comparison in calculation time between the two models, it should be checked whether the number of elements used in the MSL pipe is optimised towards temperature representation in the pipe. This is difficult because of the variations in water velocity in the pipes: a different velocity means a change in the Courant number, which is the most important parameter in choosing the spatial and temporal discretization steps. This shows an important advantage of the plug flow model, namely the independence of a grid and time step, for as long as the fluid does not exit a pipe segment in the same time step where it entered.

The downward temperature peak of the *plug flow pipe* after around 120 h (see Fig. 9) is explained by the memory of the pipe. Depending on the length of the zero flow period, the model calculates the temperature decrease of the fluid, however without accounting for the axial diffusion of heat that may have taken place. The longer the standstill period, the closer the water temperature is to the outside temperature. Therefore, there is a lowered outlet temperature during the time that it takes to completely empty the pipe segment where the fluid stood still. This also explains the upward peaks between the 48th and 72th hour, where the mass flow peak is so high that the inlet temperature is very close to the supply temperature at the producer all of a sudden.

Furthermore, it may well be that there is a bypass during flow standstill. This bypass allows supply water to flow directly to the return side without being cooled at the substation. The purpose of this bypass is to prevent the cooling down of the water in a pipe when there is no heat demand. It is however not known whether such a bypass is in place and it cannot be deduced from the measurements.

The next stage of our research will include scaling-up studies where the benefit of the plug flow model with respect to the MSL model is examined in simulations with much larger numbers of pipes and consumers. Based on the results of this paper, considerable speed-up while maintaining, or even improving, the accuracy is expected.

5. Conclusion

This paper has shown the implementation and validation of a new open source pipe model for thermal networks. Although the model is implemented in Modelica, it is applicable independent of the modelling language. Together with already existing pressure drop models from the IBPSA Modelica library, in which the model is embedded, it is possible to represent complex thermal network behaviour, including flow reversal, zero mass flow rate and varying inlet temperatures.

The validation exercise has shown that the model is accurate with respect to the measurement uncertainty. Slight discrepancies during temperature steps remain and can be explained by the inaccuracy of the mass flow rate measurements. Extensions regarding diffusion and mixing at a temperature front and mixing at standstill could further improve the model quality.

The comparison with a pipe model that uses multiple control volumes shows good correspondence, and the ability to represent fast dynamics is better. The plug flow model has a faster simulation time than both of the discretized model implementations. Major advantages over the element model are the fact that the grid size and time step do not have to be adapted to the flow velocity, and that there is no numerical diffusion.

Acknowledgement

The authors gratefully acknowledge the support of the European Union, the European Regional Development Fund ERDF, Flanders Innovation & Entrepreneurship and the Province of Limburg through the project *'Towards a Sustainable Energy Supply in Cities'* (EFRO SALK 936); the Federal Ministry for Economic Affairs and Energy in Germany for funding the project *'Effizienz und Betriebssicherheit von Energiesystemen mit saisonaler Energiespeicherung in Aquiferen für Stadtquartiere'* (BMWi 03ESP409C). This research was furthermore supported by the Assistant Secretary for Energy Efficiency and Renewable Energy, Office of Building Technologies of the U.S. Department of Energy, under Contract No. DE-AC02-05CH11231, and for the Austrian Institute of Technology (AIT) partner, with funds from the Climate and Energy Fund and implemented in line with the "IEA Ausschreibung 2013" programme, project number 843149. For AEE INTEC, the research has been conducted within the framework of the Research Studio Austria "EnergySimCity".

This research emerged from the Annex 60 project, an international project conducted under the umbrella of the International Energy Agency (IEA) within the Energy in Buildings and Communities (EBC) Programme. Annex 60 developed and demonstrated new generation computational tools for building and community energy systems based on Modelica, Functional Mockup Interface and BIM standards.

Finally, the authors would like to thank Keith O'Donovan for proofreading the manuscript and for his helpful comments.

References

[1] Lund H, Werner S, Wiltshire R, Svendsen S, Eric J, Hvelplund F, et al. 4th Generation district heating (4GDH) integrating smart thermal grids into future sustainable energy systems. Energy 2014;68:1–11.
[2] Connolly D, Lund H, Mathiesen B, Werner S, Möller B, Persson U, Boermans T, Trier D, Østergaard P, Nielsen S, et al. Heat roadmap Europe: combining district heating with heat savings to decarbonise the EU energy system. Energy Policy 2014;65:475–89.
[3] Persson U, Möller B, Werner S. Heat roadmap Europe: identifying strategic heat synergy regions. Energy Policy 2014;74:663–81.
[4] Schweiger G, Rantzer J, Ericsson K, Lauenburg P. The potential of power-to-heat in Swedish district heating systems. Energy February 2017 [in press]. http://dx.doi.org/10.1016/j.energy.2017.02.075.
[5] Böttger D, Götz M, Lehr N, Kondziella H, Bruckner T. Potential of the power-to-heat technology in district heating grids in Germany. Energy Proc 2014;46:246–53.
[6] Wetter M, Fuchs M, Grozman P, Helsen L, Jorissen F, Lauster M, et al. IEA EBC ANNEX 60 Modelica library – an international collaboration to develop a free open-source model library for buildings and community energy systems. In: Proceedings of BS2015: 14th Conference of International Building Performance Simulation

Association (Hyderabad, India); 2015. p. 395–402.
[7] Modelica Association. Modelica® – a unified object-oriented language for systems modeling language specification version 3.3 revision 1; 2014.
[8] Dynasim AB. Dymola user's manual; 2004.
[9] Wetter M, Bonvini M, Nouidui TS. Equation-based languages – a new paradigm for building energy modeling, simulation and optimization. Energy Build 2016;117:290–300.
[10] Casella F. Simulation of large-scale models in Modelica: state of the art and future perspectives. Proceedings of the 11th international Modelica conference, Versailles, France, September 21–23, 2015. Linkoping University Electronic Press; 2015.
[11] Franz G, Grigull U. Wärmeverluste von beheizten Rohrleitungen im Erdboden. Heat Mass Transf 1969;2(2):109–17.
[12] Menyhárt J, Homonnay G. Wärmeverluste der modernen Heisswasser-Fernleitungen. Period Polytech 1976;20(1):3–17.
[13] Eskilson P. Thermal analysis of heat extraction boreholes. PhD thesis. Sweden: University of Lund; 1987.
[14] Bennet J, Claesson J, Hellström G. Multipole method to compute the conductive heat flows to and between pipes in a composite cylinder. Notes Heat Transf 1987;3(January).
[15] Hellström G. Ground heat storage – thermal analyses of duct storage systems. PhD thesis. Sweden: University of Lund; 1991.
[16] Claesson J, Hellström G. Multipole method to calculate borehole thermal resistances in a borehole heat exchanger. HVAC & R Res 2011;17(6):895–911.
[17] Wallentén P. Steady-state heat loss from insulated pipes. PhD thesis. Sweden: Lund Institute of Technology; 1991.
[18] Leonard BP. A stable and accurate convective modelling procedure based on quadratic upstream interpolation. Comput Methods Appl Mech Eng 1979;19(1):59–98.
[19] Bennonysson A. Dynamic modelling and operation optimization of district heating systems. PhD thesis. Denmark: Technical University of Denmark (DTU); 1991.
[20] Benonysson A, Bøhm B, Ravn H. Operational optimization in a district heating system. Energy Convers Manage 1995;36(5):297–314.
[21] Pálsson H, Larsen HV, Bøhm B, Ravn HF, Zhou J. Equivalent models of district heating systems for on-line minimization of operational costs of the complete district heating system. Tech rep 1323. Technical University of Denmark; 1999.
[22] Bøhm B. On transient heat losses from buried district heating pipes. Int J Energy Res 2000;24(15):1311–34.
[23] Larsen HV, Pálsson H, Bøhm B, Ravn HF. Aggregated dynamic simulation model of district heating networks. Energy Convers Manage 2002;43(8):995–1019.
[24] Larsen HV, Bøhm B, Wigbels M. A comparison of aggregated models for simulation and operational optimisation of district heating networks. Energy Convers Manage 2004;45(7):1119–39.
[25] Vesterlund M, Dahl J. A method for the simulation and optimization of district heating systems with meshed networks. Energy Convers Manage 2015;89:555–67.
[26] Gabrielaitiene I, Bøhm B, Sunden B. Modelling temperature dynamics of a district heating system in Naestved, Denmark – a case study. Energy Convers Manage 2007;48(1):78–86.
[27] Gabrielaitiene I. Numerical simulation of a district heating system with emphasis on transient temperature behaviour. In: Environmental engineering – the 8th international conference, (Vilnius, Lithuania); 2011. p. 747–54.
[28] Sandou G, Font S, Tebbani S, Hiret A, Mondon C. Predictive control of a complex district heating network. In: Proceedings of the 44th IEEE conference on decision and control; 2005. p. 7372–7.
[29] Stevanovic VD, Zivkovic B, Prica S, Maslovaric B, Karamarkovic V, Trkulja V. Prediction of thermal transients in district heating systems. Energy Convers Manage 2009;50(9):2167–73.
[30] Grosswindhager S, Voigt A, Kozek M. Linear finite-difference schemes for energy transport in district heating networks. In: Proceedings of the 2nd international conference on computer modelling and simulation; 2011. p. 5–7.
[31] Dalla Rosa A, Li H, Svendsen S. Method for optimal design of pipes for low-energy district heating, with focus on heat losses. Energy 2011;36(5):2407–18.
[32] Dalla Rosa A, Li H, Svendsen S. Modeling transient heat transfer in small-size twin pipes for end-user connections to low-energy district heating networks. Heat Transf Eng 2013;34(4):372–84.
[33] Ben Hassine I, Eicker U. Impact of load structure variation and solar thermal energy integration on an existing district heating network. Appl Therm Eng 2013;50(2):1437–46.
[34] Guelpa E, Toro C, Sciacovelli A, Melli R, Sciubba E, Verda V. Optimal operation of large district heating networks through fast fluid-dynamic simulation. Energy 2016;102:586–95.
[35] Guelpa E, Sciacovelli A, Verda V. Thermo-fluid dynamic model of large district heating networks for the analysis of primary energy savings. Energy 2017. http://dx.doi.org/10.1016/j.energy.2017.07.177. [in press].
[36] Kauko H, Kvalsvik KH, Rohde D, Hafner A, Nord N. Dynamic modelling of local low-temperature heating grids: a case study for Norway. Energy 2017. http://dx.doi.org/10.1016/j.energy.2017.07.086. [in press].
[37] Jie P, Tian Z, Yuan S, Zhu N. Modeling the dynamic characteristics of a district heating network. Energy 2012;39(1):126–34.
[38] Zheng J, Zhou Z, Zhao J, Wang J. Function method for dynamic temperature simulation of district heating network. Appl Therm Eng 2017;123:682–8.
[39] Skoglund T, Årzén KE, Dejmek P. Dynamic object-oriented heat exchanger models for simulation of fluid property transitions. Int J Heat Mass Transf 2006;49(13–14):2291–303.
[40] Skoglund T, Dejmek P. A dynamic object-oriented model for efficient simulation of fluid dispersion in turbulent flow with varying fluid properties. Chem Eng Sci 2007;62(8):2168–78.
[41] Velut S, Tummescheit H. Implementation of a transmission line model for fast simulation of fluid flow dynamics. In: Proceedings 8th Modelica conference, (Dresden); 2011. p. 446–453.
[42] Giraud L, Baviere R, Vallée M, Paulus C. Presentation, validation and application of the DistrictHeating Modelica library. In Proceedings 11th Modelica conference, (Versailles, France); September 2015. p. 79–88.
[43] Giraud L, Merabet M, Baviere R, Vallée M. Optimal control of district heating systems using dynamic simulation and mixed integer linear programming. In: Proceedings of the 12th international Modelica conference, (Prague, Czech Republic); 2017. p. 141–50.
[44] Van den Bossche G. Lokale temperatuurverhoging versus tijdmodulatie in lage temperatuur warmtenetten. Master thesis. Belgium: KU Leuven; 2015.
[45] Sartor K, Thomas D, Dewallef P. A comparative study for simulating heat transport in large district heating networks. In: Proc ECOS 2015 – 28TH int conf effic COST, optim simul environ IMPACT ENERGY syst; 2015.
[46] Sartor K, Dewalef P. Experimental validation of heat transport modelling in district heating networks. Energy 2017 [in press, corrected proof]. https://doi.org/10.1016/j.energy.2017.02.161.
[47] Oppelt T, Urbaneck T, Gross U, Platzer B. Dynamic thermo-hydraulic model of district cooling networks. Appl Therm Eng 2016;102:336–45.
[48] Schweiger G, Larsson P-O, Magnusson F, Lauenburg P, Velut S. District heating and cooling systems – framework for Modelica-based simulation and dynamic optimization. Energy 2017 [in press]. http://dx.doi.org/10.1016/j.energy.2017.05.115.
[49] Schweiger G, Runvik H, Magnusson F, Larsson P-O, Velut S. Framework for dynamic optimization of district heating systems using OPTIMICA compiler toolkit. In: Proceedings of the 12th international Modelica conference, Prague; 2017.
[50] van der Heijde B, Aertgeerts A, Helsen L. Modelling steady-state thermal behaviour of double thermal network pipes. Int J Therm Sci 2017;117:316–27.
[51] Cvema F. ASM ready reference: thermal properties of metals. ASM International; 2002.
[52] Nellis G, Klein S. Heat transfer. Cambridge University Press; 2009.
[53] Kaarup Olsen P, Holm Christiansen C, Hofmeister M, Svendsen S, Thorsen J-E, Gudmundsson O, et al. Guidelines for low-temperature district heating. Tech rep; April 2014.
[54] Skagestad B, Mildenstein P. District heating and cooling connection handbook. Tech rep; 1999.
[55] Woods P. Heat networks: code of practice for the UK. Tech rep; 2014.
[56] Kristjansson H, Bøhm B. Optimum design of distribution and service pipes. Tech rep. Danfoss; 2006.
[57] de Boer S, Korsman J, Smits I. Long term heat loss of plastic polybutylene piping systems. In: The 11th international symposium on district heating and cooling, August 31 to September 2, 2008, Reykjavik, ICELAND, no. 1; 2008. p. 1–8.